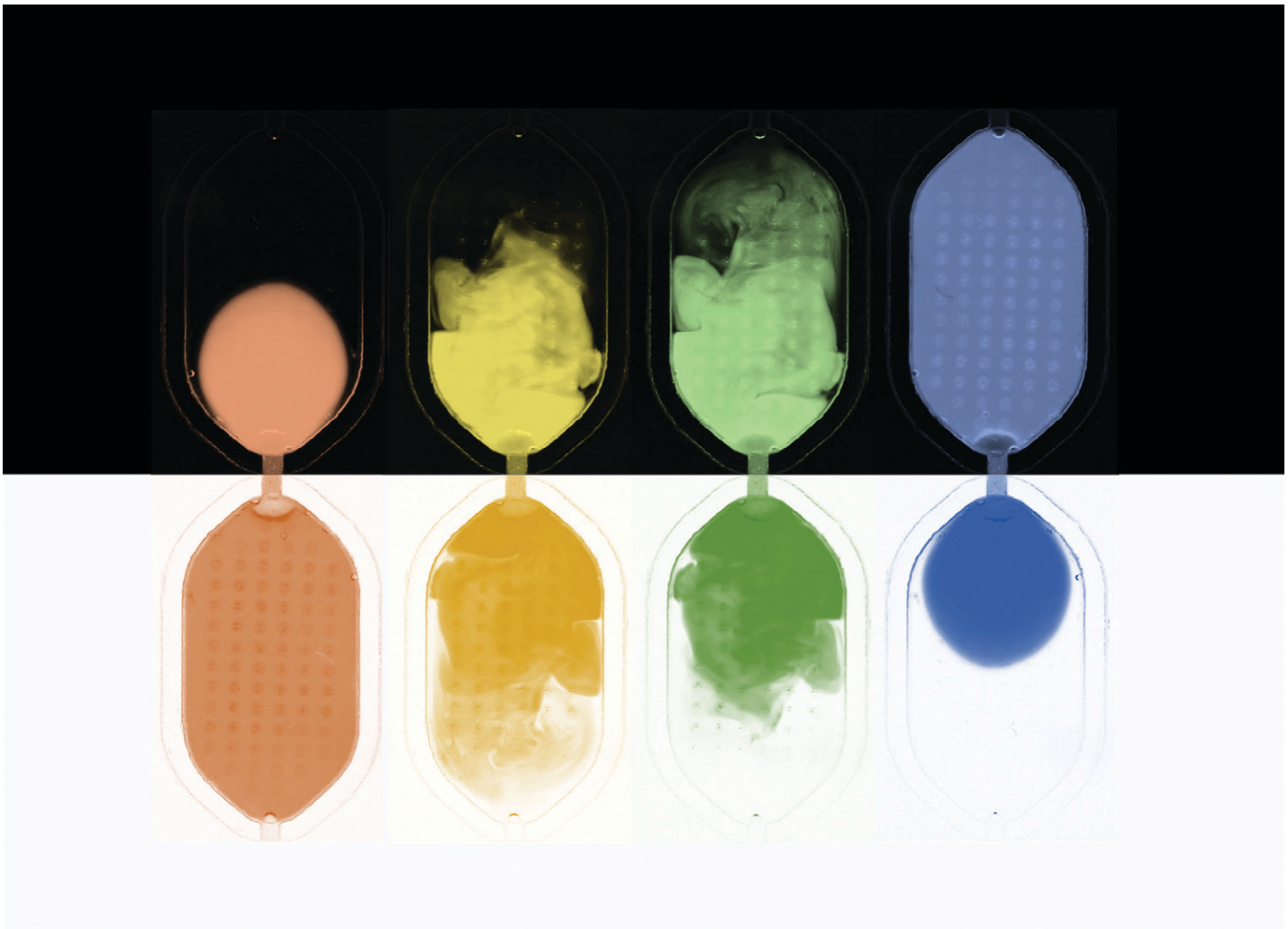

Showcasing research from the Clinical Microfluidics Laboratory of Dr Kersaudy-Kerhoas, School of Engineering and Physical Sciences, Heriot-Watt University, UK.

Versatile hybrid acoustic micromixer with demonstration of circulating cell-free DNA extraction from sub-ml plasma samples

A low-cost and easy to implement acoustic micromixer compatible with multiple fabrication technologies that can provide vigorous and efficient mixing, was developed and demonstrated on cell-free DNA purification from human plasma, using a magnetic bead based commercial kit. The acoustic mixer delivered up to a ten-fold increase in capture efficiency, compared to the manual bench technique.

As featured in:

See Maïwenn Kersaudy-Kerhoas *et al.*, *Lab Chip*, 2020, **20**, 741.

ROYAL SOCIETY OF CHEMISTRY

rsc.li/loc

Registered charity number: 207890

Lab on a Chip

PAPER

View Article Online
View Journal | View Issue

Cite this: *Lab Chip*, 2020, **20**, 741

Versatile hybrid acoustic micromixer with demonstration of circulating cell-free DNA extraction from sub-ml plasma samples†

Alvaro J. Conde, [ab] Ieva Keraite,[ab] Alfredo E. Ongaro [abc] and Maïwenn Kersaudy-Kerhoas *[ab]

Received 14th November 2019,
Accepted 9th January 2020

DOI: 10.1039/c9lc01130g

rsc.li/loc

Acoustic micromixers have attracted considerable attention in the last years since they can deliver high mixing efficiencies without the need for movable components. However, their adoption in the academic and industrial microfluidics community has been limited, possibly due to the reduced flexibility and accessibility of previous designs since most of them are application-specific and fabricated with techniques that are expensive, not widely available and difficult to integrate with other manufacturing technologies. In this work, we describe a simple, yet highly versatile, bubble-based micromixer module fabricated with a combination of low-cost rapid prototyping techniques. The hybrid approach enables the integration of the module into practically any substrate and the individual control of multiple micromixers embedded within the same monolithic chip. The module can operate under static and continuous flow conditions showing enhanced mixing capabilities compared to similar devices. We show that the system is capable of performing cell-free DNA extractions from small volumes of blood plasma (≤500 μl) with up to a ten-fold increase in capture efficiency when compared to control methods.

Introduction

Micromixers are essential components in microfluidic devices which have a direct impact on the efficiency and sensitivity of assays.[1] However, mixing in microfluidics is also one of the main challenges since inertial effects are almost irrelevant due to the low Reynolds number in which these systems usually operate. Consequently, researchers endeavour to counterweigh the limits of purely diffusive mixing by introducing structures or active mechanisms that disturb the flow with the ultimate objective of diminishing the striation length and increasing the area across which diffusion takes place, thus enabling a rapid homogenisation of the solution.[2]

Sound field driven, or acoustic, micromixers have attracted considerable attention in the last years since they can deliver high mixing efficiencies without the integration of fragile movable components in opposition to their magnetic counterparts.[1,3–5] Surface acoustic wave (SAW) micromixers have shown to be promising, but they require the integration of microelectrodes on piezoelectric substrates which can lead to biocompatibility issues and can drive the fabrication costs up.[6] Ultrasonic actuation has been shown to provide efficient mixing; however, significant heat is generated during the operation, carrying the need for bulky active cooling mechanisms.[7] Other types of acoustic mixers can be implemented based on the vibration of membranes;[8] sharp-edge structures;[9] micropillars[10] and cilia.[11] Nevertheless, all of these devices are fabricated using intricate and laborious techniques which are not widely available and can be cost-prohibitive for many groups.

A surprisingly simple, yet powerful concept, is the acoustic actuation of air bubbles trapped within miniaturised devices. This method has been posed to be the "holy grail" for achieving fast (down to milliseconds) convective mixing at microscale lengths.[12] In contrast to mechanical mixers, the microstreaming flow generated by the oscillating bubbles can be driven well beyond the Stokes boundary layer, producing efficient mixing even when dealing with highly viscous fluids.[13] Moreover, the actuators for this kind of micromixers are generally economical, low-power and have a reduced footprint.

Researchers have previously developed a variety of highly efficient bubble-based micromixers,[13–24] but most of them are fabricated using (SU-8 mould) soft-lithography, a highly manual and laborious technique that requires specialised equipment and is difficult to mass-manufacture. Furthermore, the total cost of microfluidic chips fabricated

[a] *Institute of Biological Chemistry, Biophysics and Bioengineering, School of Engineering and Physical Science, Heriot-Watt University, Edinburgh, UK. E-mail: m.kersaudy-kerhoas@hw.ac.uk*
[b] *Infection Medicine, Edinburgh Medical School, College of Medicine and Veterinary Medicine, The University of Edinburgh, Edinburgh, UK*
[c] *Department of Civil, Environmental, Aerospace and Materials Engineering (DICAM), University of Palermo, Palermo, Italy*
† Electronic supplementary information (ESI) available. See DOI: 10.1039/c9lc01130g

using this technique is usually underestimated and can be unaffordable for many research groups.[25] Other authors have investigated the use of thermoplastics and other fabrication techniques, such as CNC micro-milling,[17,18] laser cutting[21] and hot embossing,[22] however they share a common limitation along with the soft-lithography-based devices: the actuator (piezoelectric transducer) has to be glued using permanent adhesives to the bulk of the chip, impeding the individual control of more than one micromixer per chip and complicating the assembly process.

In this paper, we describe a novel bubble-based acoustic micromixer module that overcomes all of the aforementioned limitations. The micromixer is fabricated using a hybrid strategy, a combination of rapid prototyping technologies that are low-cost and widely available; it is, for example, possible to order all the necessary parts for their fabrication by mail.[25] The hybrid strategy enables the incorporation of the module into practically any substrate and the capability to individually address multiple micromixers integrated within the same monolithic chip. The results show that the micromixer can perform effective homogenisation of two solutions, in continuous and static flow conditions, with enhanced performances compared to similar bubble-based micromixers. Additionally, the mixer can operate over a broad range of volumes (10–800 μl) in static flow conditions, something unique to our system. Finally, we validate the capability of the system to accomplish efficient circulating cell-free DNA (cfDNA) extractions from small volumes of blood plasma samples using a commercial kit based on magnetic beads.

Experimental

Design

In order to tackle the limitations of previously reported bubble-based micromixers and taking inspiration from a previously reported hybrid microfluidic device,[26] we propose the hybrid approach illustrated in Fig. 1A. This hybrid design combines a substrate (hard polymer) with a slab (soft polymer). The substrate contains the mixing chamber and the microfluidic channels, while the slab contains the structures (pockets) necessary to trap the air bubbles (Fig. 1B) that will perform the microstreaming when acoustically stimulated (Fig. 1C).

A hermetic seal is formed when the deformable slab is mechanically compressed against the complementary structure on the mixing chamber. This compression force can be given by 1) the piezoelectric actuator when tightened to the chip *via* a matching frame and four screws (Fig. S1A†), or 2) by an auxiliary chip layer (Fig. S1B†). The first configuration allows for fast design iterations and the reuse of the components, while the second one enables the manufacturing of closed disposable chips. In both configurations, the acoustic energy is concentrated on the slab while much less energy is transferred to the substrate, enabling thus high mixing efficiencies and the individual control of several micromixers per chip as confirmed by the results. All micromixers in this work were fabricated following the first configuration. This solution provides tight sealing up to 100 kPa of pressure (burst test experiments performed as in the ref. 27). An example of a micromixer chip manufactured following the second configuration is shown in Fig. S2.†

Microfluidic chips fabrication

Microfluidic chips for the mixing characterisation and cfDNA experiments were fabricated from cell-cast polymethyl methacrylate (PMMA) sheets (Clarex, Nitto Jushi Kogyo) using a previously reported rapid prototyping method.[27] Briefly, after laser cutting the desired shapes using a CO_2 laser cutter (Epilog Mini 18, Epilog, USA), PMMA layers were cleaned with a clean-room tissue soaked in ethanol and blown-dry with compressed air to remove dust. 80 μl of ethanol was spread between each of the layers using a pipette just before bonding. This allows for the partial melting of a superficial layer and the formation of a strong bond between the PMMA elements even if operating below PMMA Tg. Immediately after the ethanol spread, the assembly was placed in custom-made aluminium alignment frames and subsequently

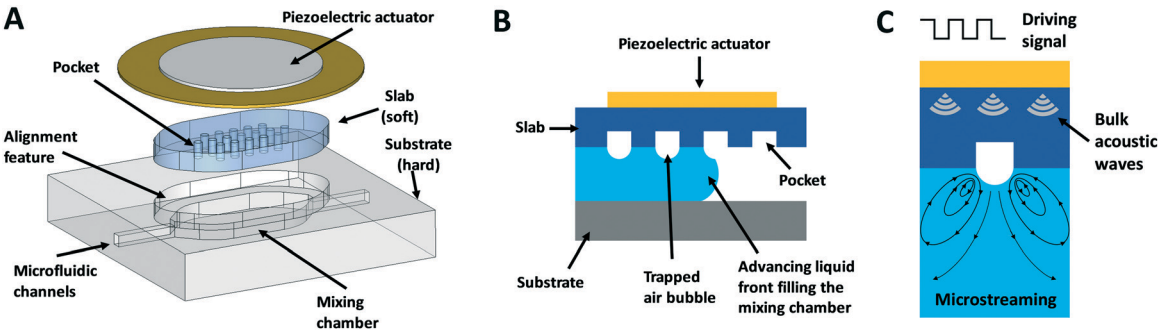

Fig. 1 A) Exploded 3D view of the hybrid micromixer concept. B) Cross-sectional schematic (not to scale) of the hybrid micromixer showing the components and the formation of the bubbles during the filling of the mixing chamber. C) Cross-sectional schematic showing a single bubble when acoustically actuated (not to scale). The acoustic waves produced by the piezoelectric disc travel through the bulk of the soft material and produce radial oscillations on the trapped air bubbles, generating strong microstreaming effects in the mixing chamber.

positioned between the plates of a heated press (PW100–37, Carver). A load of 2 metric tons was applied for 3 minutes at 70 °C. After the bonding, the chips were blow dry with compressed air and stored until use. A photograph of a fabricated PMMA microfluidic chip is shown in Fig. 2A. More details and photographs of all the chips used for the mixing characterisation experiments are shown in Fig. S3.†

To demonstrate compatibility with other manufacturing technologies, 3D-printed chips were manufactured by fused deposition modelling (FDM) and stereolithography (SLA) technologies. FDM chips were fabricated using a commercial FDM printer (Mega i3, Anycubic) using a polylactic acid (PLA) filament (clear 1.75 mm filament, verbatim). The following printing parameters were used: extrusion temperature: 210 °C, bed temperature: 60 °C, printing speed: 30 mm s^{-1}. For visualisation purposes, an optical window at the bottom of the chamber was created by glueing (Super Glue, 3M) a piece of 0.2 mm thick PMMA that was cut using a laser cutter. This piece can also be obtained by manually cutting the thin PMMA sheet with scissors. A photograph of a fabricated and fully assembled FDM micromixer chip is shown in Fig. S4A.† SLA chips were fabricated using a commercial SLA 3D printer (form 2, Formlabs) using a clear resin (Clear V4, Formlabs). After removing the uncured resin by rinsing the parts in pure isopropanol, the parts were cured in a UV crosslinker (CX-2000, UVP/Analytik Jena) for 30 min and subsequently heat-cured in an oven at 60 °C for 1 hour. The UV curing is not mandatory although recommended by the manufacturer. The same strategy followed for the FDM chips was used to create the optical window at the bottom of the mixing chamber. A photograph of a fabricated and fully assembled SLA micromixer chip is shown in Fig. S4B.†

Slabs fabrication

Slabs were fabricated by casting polydimethylsiloxane (PDMS) onto SLA-3D printed moulds. The moulds contain an array of posts (Fig. S5A†) that serve as negative structures for the formation of the pockets after the casting process. The moulds were fabricated following the same methods as described for the SLA microfluidic chips. A diagram of the casting process is shown in Fig. S5B.† Briefly, a silicone elastomer (Sylgard 184, Dow Chemical Company) was thoroughly mixed in 1 : 10 ratio, degassed in a vacuum chamber and subsequently poured over the clean moulds. Immediately after the casting, a small 0.2 mm thick PMMA piece was placed on top of the moulds to generate a flat and polished surface on the cured PDMS slab. This particular surface is necessary to ensure intimate contact between the slab and the piezoelectric disc and to avoid the use of coupling mediums. The casted moulds were left to cure overnight at room temperature. After this period, the PMMA piece was removed and an additional curing step of 2 hours at 60 °C was performed. Finally, the slabs were carefully peeled from the mould using tweezers and stored until use. A photograph of one of the obtained PDMS slabs is shown in Fig. 2B. More details and photographs of all the PDMS slabs can be found in Fig. S3.†

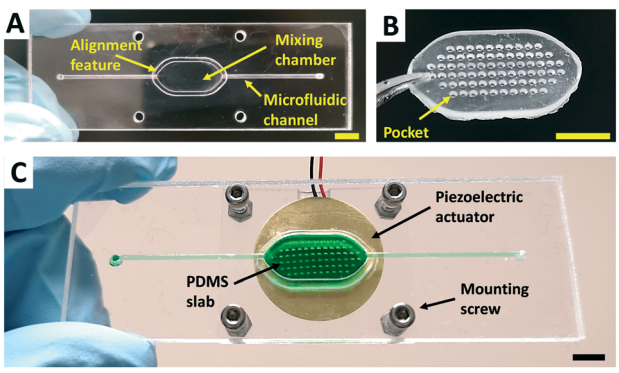

Fig. 2 A) Photograph of a fabricated PMMA microfluidic chip for the characterisation of the micromixer in static flow conditions. B) Photograph of a fabricated PDMS slab. C) Photograph of a fully assembled micromixer module in a PMMA microfluidic chip loaded with green food dye for visualisation purposes. Scale bars are 5 mm.

Piezoelectric actuators and driver

Piezoelectric diaphragms with different diameters were used (15 mm 7BB-15-6L0, 20 mm 7BB-20-6 and 27 mm 7BB-27-4, Murata Electronics). Photographs of these devices can be found in Fig. S3.† A function generator (TG215, Thurlby Thandar Instruments) was used as a driver. This generator can work with voltages up to 20 Vp–p. For higher voltages, we used a 1 : 3 : 10 turn ratio audio transformer (NTE10/3, Neutrik) connected with the signal generator.

Image acquisition and analysis

Videos and images for the mixing characterisation experiments were acquired using digital microscopes with white light (AM7013MZT, Dino-Lite) and with fluorescence capability (AM4115T-GFBW, Dino-Lite). Images and videos were captured using the software DinoCapture 2.0 (Dino-Lite) and processed using ImageJ.

Plasma samples and cell-free DNA extraction

Blood was drawn from healthy volunteers in EDTA tubes and plasma immediately separated by double centrifugation at low speed (4000*g*) for 10 min and high speed (12 000*g*) for 10 min. The plasma samples were used for cfDNA extraction shortly after separation without any freeze–thaw cycles to avoid any potential degradation of the DNA fragments.

To extract the cfDNA from plasma, we used the magnetic beads-based MagMAX cfDNA isolation kit (ThermoFisher Scientific) following the manufacturer's recommended protocol for the controls (bench) and a modified protocol for the microfluidic assays as shown in Table S1.†

Special PMMA microfluidic chips with a mixing volume of 255 µl and 1100 µl were fabricated following the same methods as described for the mixing characterisation experiments. As shown in Table S1,† these volumes are

necessary for the processing of 100 μl and 500 μl of plasma respectively. A larger PDMS slab was fabricated for the 1100 μl chip. Photographs of the chips and the slabs used for these experiments are shown in Fig. S8.† Before the cfDNA experiments, the chips were coated with a solution of 2% bovine serum albumin (Sigma Aldrich) in 1× PBS (ThermoFisher Scientific) for 5 minutes at room temperature in order to avoid non-specific adsorption of the cfDNA fragments to the chip walls. Immediately after, the chips were washed with nuclease-free water (QIAGEN) and allowed to dry for a couple of minutes before running the experiments.

To demonstrate the magnetic beads disaggregation capabilities, two stacked magnets (5 mm diameter, 2 mm thick, N804RS, Eclipse Magnetics) were positioned on top of the piezoelectric disc roughly in the centre of the chamber as shown in Fig. S9A.† For the cfDNA capture experiments, we used a more powerful magnet (5 × 10 × 25 mm, N818RS, Eclipse Magnetics) that was positioned on top of the piezoelectric disc (Fig. S9B†) when required by the protocol to perform the capture of the magnetic beads.

Cell-free DNA quantification and fragment analysis

Real-time quantitative PCR (RT-qPCR) was performed using 2× Power SYBR® Green PCR Master Mix (Thermo Fisher Scientific) to quantify total cfDNA by amplifying LINE-1 (long interspersed nuclear elements) target of 90 bp. The total reaction volume was 12.5 μl with a final concentration of each primer of 200 μM (LINE FW 5′-TGCCGCAATAAACA TACGTG-3′, LINE RV 5′-GACCCAGCCATCCCATTAC-3′) and 1 μl cfDNA elution.[28] Thermal cycling conditions involved a 10 min cycle at 95 °C followed by 40 cycles with 15 s at 95 °C and 60 s at 60 °C. Samples were amplified in duplicate using Mx3005P qPCR system (Agilent). A melting curve was performed as a control measure for nonspecific amplification. The standard curve for absolute quantification of cfDNA was created with commercially available human genomic DNA (Bioline) with a linear range over 5 orders of magnitude. Linear regression analysis was done in MxPro qPCR software ($R^2 > 0.98$).

CfDNA fragment size analysis was performed using the High Sensitivity D5000 ScreenTape assay on the Agilent 4200 TapeStation system. Data were analysed with TapeStation Analysis Software Version A.02.02 (SR1).

Results and discussion

Resonant frequency

The intensity of the streaming generated by the oscillating bubbles is mainly a function of the applied voltage and frequency. The frequency in which the intensity of the streaming is maximum is called resonant or optimal frequency. This frequency is mainly a function of geometrical bubble parameters and can be theoretically estimated.[29] However, the resonant frequency can also be experimentally determined by visual observation due to the limited predictability of the models[16] and fabrication tolerances of the 3D printed moulds. Briefly, a frequency sweep is performed using a signal generator, and the microstreaming phenomenon is observed under the digital microscope. To help with this qualitative assessment, fluorescent microparticles (5 μm beads FITC-marked, Sigma Aldrich) were suspended in deionised water (DW) and loaded into the different micromixing chambers. Micrographs of a 100 μl micromixing chamber (Fig. S3C†) with no actuation and actuation at the resonant frequency are shown in Fig. 3A. A video demonstrating this process can be found in the ESI.† The main resonant frequency for all the fabricated micromixers was 4.2 ± 0.5 kHz.

Mixing under static-flow conditions

Most of the reported micromixers are designed to operate continuously by disrupting the laminar flow streams to be mixed; however, there are many microfluidic applications that require the mixing of fluids under static-flow conditions. This is especially important in point-of-care (POC) applications where stored reagents must be mixed in confined volume chambers. To demonstrate the capability of the presented system to perform these actions, microfluidic chips integrating mixing chambers with different volumes (10–800 μl) were fabricated. Photographs of these chips are shown in Fig. S3† (A–C, E, I and J). The chips were prefilled with DW and then a solution of fluorescein in DW was injected until approximately half of the chamber was filled. Immediately after filling, the piezoelectric was turned on and the mixing effect observed. The mixing time is calculated by analysing the videos with ImageJ and finding the time in which the mixing is no longer improved through a cut line (averaged width 20 px) placed across the chamber as shown in Fig. S6.† A video of this process for a 200 μl chamber can be found in the ESI.† The assays were done by triplicate and filling from both sides.

As shown in Fig. 3B, the hybrid micromixer can effectively mix the samples in less than 35 seconds across all the volume range. These mixing times are comparable or better to similar previous static-flow bubble-based micromixers; however, these devices operate in significantly smaller volumes and have the drawback of the glued piezoelectric disc.[16–19] Moreover, the hybrid micromixer can perform efficient mixing over a wide range of volumes, something unique to our system. As a comparison, diffusion only mixing takes approximately 36 hours to homogenise the species in a 200 μl chamber (Fig. S7†).

From the results shown in Fig. 3B, we have also observed the appearance of a valley in the mixing time for chamber volumes around 100–200 μl. We believe that this phenomenon could be owed to a synergistic interaction between the microstreaming forces and associated secondary flows[30] from different bubbles that, as a consequence, generate additional flows that further improve the mixing efficiency for these particular geometrical configurations.

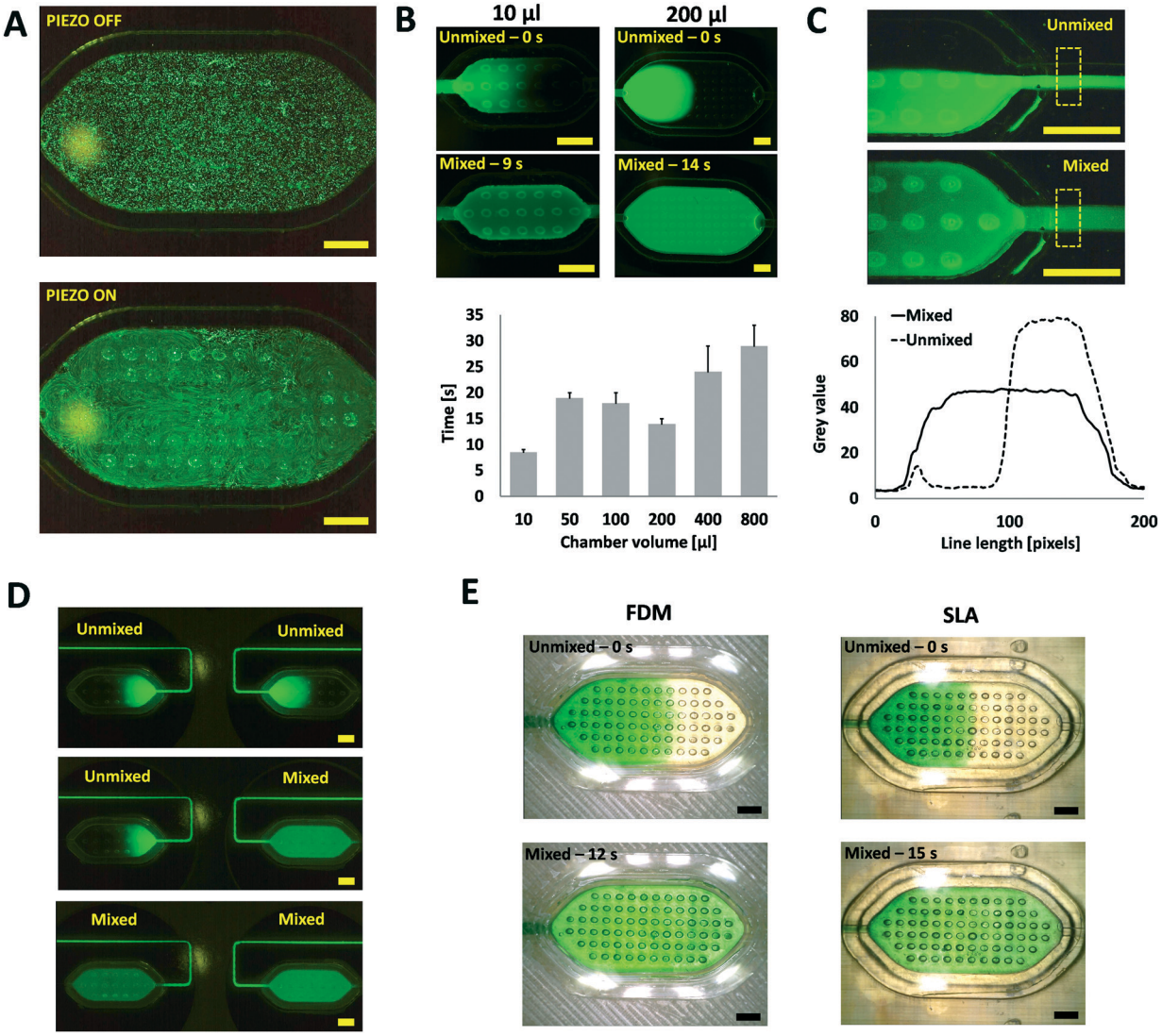

Fig. 3 A) Micrographs of a mixing chamber integrated into a PMMA chip loaded with fluorescent microparticles showing the microstreaming effect produced by the oscillating bubbles. B) Top: Micrographs showing a 10 µl and a 200 µl mixing chambers integrated into PMMA chips under static flow conditions before and after mixing. Bottom: Mixing time as a function of the chamber volume. C) Top: Micrograph of the continuous flow mixing chamber integrated into a PMMA chip before and after mixing (total flow rate of 200 µl min^{-1}). Bottom: Plot of the average pixel grey value along the area highlighted in the yellow dashed rectangle in the top micrographs. D) A sequence of micrographs demonstrating the capability to individually address two different micromixers integrated within the same PMMA chip. E) Micrographs of 200 µl mixing chambers integrated into chips fabricated with fused deposition modelling (FDM) and stereolithography (SLA) 3D printing technologies before and after mixing. Comparable performances to the PMMA laminated devices were obtained. A 15 VRMS square wave was used to stimulate the piezoelectric discs for all the experiments. Scale bars are 2 mm.

Mixing under continuous-flow conditions

To study the performance of the micromixer under continuous-flow conditions, microfluidic chips with two inlets and a mixing chamber (positioned immediately after the merging point of the two inlet channels) were fabricated (Fig. S3D†). A solution of fluorescein in DW and DW were flown at 100 µl min^{-1} per channel using two syringe pumps (AL-1000HP, World Precision Instruments). After the laminar flow was established, the piezoelectric was turned on and off, and the mixing process observed and recorded using a fluorescent digital microscope. A video of this experiment can be found in the ESI.† Snapshots extracted from these videos (corresponding to the area marked in yellow at the top in Fig. 3C) were analysed in ImageJ to evaluate mixing efficiency. Briefly, cut lines (averaged width 100 px) were positioned at the outlet of the mixing chamber (dashed yellow rectangle in Fig. 3C, top) and the grey value of the pixels plotted as shown at the bottom in Fig. 3C.

The intensity profile showed in Fig. 3C (bottom) indicates that (~1 second) after the piezoelectric is turned on, a uniform grayscale distribution across the width of the channel is observed, suggesting the complete homogenisation of the species. In the presented

configuration, the system can provide efficient mixing from no flow rate (static flow reported earlier) up to a total flow rate of 200 μl min^{-1} (12 ml h^{-1}), which is significantly higher than results from previous similar devices.[14,15,20–23] The system geometrical configuration could be optimised to enable the homogenisation of higher flow rates.

Integration of multiple individually-addressable mixers on the same chip

A common disadvantage of previously reported bubble-based micromixers is that they cannot be controlled individually within the same monolithic chip. To demonstrate that our system overcomes this limitation, we fabricated a PMMA monolithic microfluidic chip integrating two independent micromixers (Fig. S3F†). For running the experiments, the same protocol as for static-flow conditions experiments was used, but the mixers were activated at different times. A video of this experiment can be found in the ESI.†

As shown in the sequence of micrographs of Fig. 3D, it is possible to individually address different micromixers integrated within the same monolithic chip. This is a clear advantage over previously reported devices where all the micromixers would be activated simultaneously as they share the same substrate.[16–19,22]

Integration of the mixer into 3D printed chips

To further demonstrate the versatility and also the accessibility of the micromixer module, we integrated and tested the micromixer in microfluidic chips (Fig. S4†) fabricated with two of the most common and widely available 3D printing technologies; fused deposition modelling (FDM) and stereolithography (SLA). Due to the limited transparency of these 3D printed materials, optical windows were added to better observe the mixing effects. The same approach used in the static-flow condition experiments was followed but using green food dye instead of fluorescein to allow the observation of the 3D printed substrates.

As shown in Fig. 3E, the hybrid module can perform efficient mixing operations without noticeable leaking on the devices fabricated with both 3D printing technologies. This capability is enabled by the hybrid nature of the concept: the slab can easily deform and adapt to any planar substrate. An important consequence of this feature is that it allows the fabrication of different micromixers by anyone with access to 3D printers or a small budget to order 3D printed components by mail.[25] This accessibility characteristic is unique to our system since all the previously reported acoustic micromixers utilise fabrication technologies that are complex and unaffordable for many.

Circulating cell-free DNA extraction

The study of circulating cfDNA is gaining interest in various biomedical disciplines, including cancer, metabolic and cardiovascular diseases, prenatal sex determination, sepsis diagnosis and exercise physiology among others. Circulating cfDNA not only provides valuable genetic information: it can also be easily obtained from the body through a minimally invasive blood draw, so-called liquid biopsy. Most of the efforts in the cfDNA field are associated with non-invasive prenatal testing of chromosomal abnormalities, cancer detection, monitoring relapse and drug resistance. In these studies, and due to the very low concentration of the interest analytes, plasma volumes between 1 ml and 5 ml are usually required. However, small volumes of plasma samples (<500 μl) can provide sufficient cfDNA concentrations for their use in different fields, such as sports medicine[31] and early fetal sex determination.[32]

Most of the current cfDNA extraction methods are based on silica membranes or silica magnetic microbeads. The latter has been reported to have a higher preference for low molecular weight DNA molecules (up to 300 bp),[33] which helps to circumvent cellular genomic DNA contamination in the sample. However, one of the main challenges of this assay is that after the application of a strong magnetic field, the beads tend to "stick" with each other, forming clusters. This issue can compromise the reproducibility and sensitivity of the assays since the cluster population can be quite heterogeneous and less surface area is available for the capture assays. Having less surface area has a significant impact in assays where the target analyte is in very low concentrations, such as cfDNA.

Acoustic microstreaming has been shown to be an efficient mechanism to disaggregate and mix microbeads in microfluidic devices.[16] To evaluate the capabilities of our system to perform these operations, we fabricated a microfluidic chip (Fig. S8A†) containing a micromixing chamber of approximately 255 μl. The chamber was loaded with a suspension of magnetic beads in DW, and a stack of neodymium magnets was used to concentrate and aggregate the beads (Fig. S9A†). After the removal of the magnetic field, the piezoelectric was turned on and the mixing effect observed under the digital microscope. As shown in Fig. 4A, the beads can be effectively disaggregated and uniformly distributed across the mixing chamber in less than 50 seconds which is similar to the results obtained in a similar device.[16] However, this previous device is fabricated using standard soft-lithography and can only mix 78 nl of sample volume. A video of this disaggregation experiment can be found in the ESI.†

After having this key disaggregation and mixing capability demonstrated, we performed a full cfDNA extraction from 100 μl (sample 1) and 500 μl (sample 2) of blood plasma samples from two different healthy donors using the micromixer and the MagMAX® Cell-Free DNA Isolation Kit. In order to accommodate the required volumes established by the manufacturer's protocol, we used the 255 μl mixing chip (Fig. S8A†) for the 100 μl plasma samples and an 1100 μl mixing chip (Fig. S8B†) for the 500 μl plasma samples. The magnetic capture set-up shown in Fig. S9† was used for these experiments.

As shown in Fig. 4B, the micromixer can capture, on average, one order of magnitude more cfDNA than the

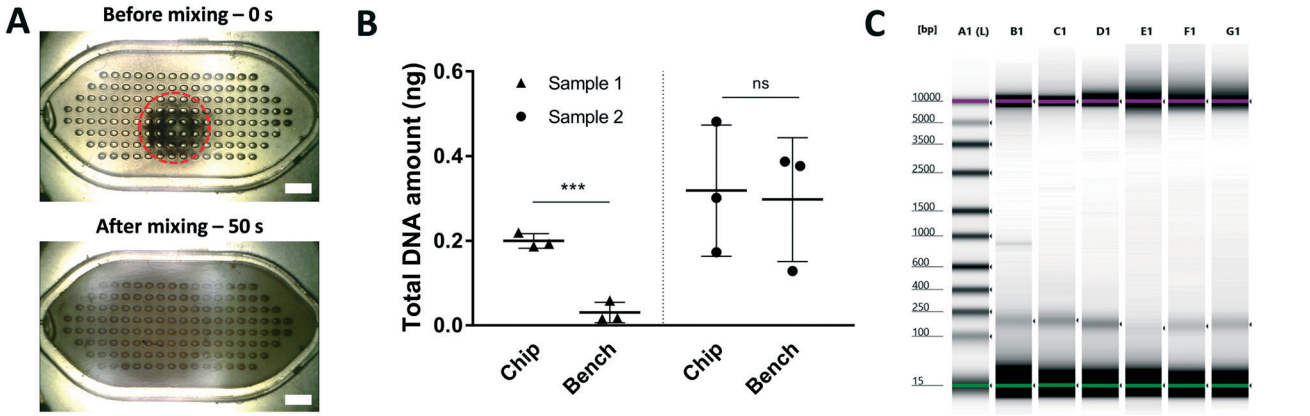

Fig. 4 A) Micrographs of a 255 μl chamber integrated into a PMMA chip demonstrating the beads disaggregation and mixing effect. The dashed red circle corresponds to the approximate silhouette of the magnetic discs stack used for aggregating the beads. Scale bars are 2 mm. B) Total cfDNA amount extracted from plasma samples using the micromixer chip and by manual bench extraction method. 100 μl (sample 1) and 500 μl (sample 2) of plasma from different blood donors were used in three independent extractions. C) Electrophoresis of cfDNA eluates from sample 2 (500 μl of plasma). Lane A1, HS D5000 ladder; lanes B1–D1, cfDNA extracted on-chip; lane E1–G1, cfDNA extracted manually on bench; green mark – lower marker, purple mark – upper marker.

manual bench protocol (control) for 100 μl of plasma sample. These results indicate that the micromixer enables enhanced capture efficiency due to the superior mixing capabilities when compared to the control methods for this volume range. To the best of our knowledge, this is the first study where a 10-fold improvement in microfluidic-based cfDNA capture efficiency is presented on 100 μl of plasma sample. These results pose the question if the current bench mixing protocols are optimal for such volumes of sample. The difference between the total DNA amounts extracted using the chip and the bench protocol are not statistically significant for the 500 μl plasma sample. We believe that this could be due to the contribution of inertial effects that promote enhanced mixing in the control method for this volume range (>1 ml). The electrophoretic results presented in Fig. 4C confirm that the captured DNA corresponds indeed to cfDNA fragments (~160 bp). The corresponding electropherograms are shown in Fig. S10.†

In summary, these results demonstrate the capability of the micromixer to perform a sample preparation assay which requires high shear forces (beads disaggregation) and high mixing efficiency (capture of a very low concentrated analyte). The mixer could be potentially integrated into micro and millifluidic cartridges with automated liquid handling operations for its implementation in POC settings. Bringing cfDNA sample preparation assays to the POC would ensure the stability and integrity of these precious molecules since the cfDNA fragments are usually short-lived, with half-lives ranging from minutes up to several hours.[34]

Conclusions

We have developed a novel bubble-based acoustic micromixer based on hybrid manufacturing. Thanks to the use of an elastomeric slab, less acoustic energy is lost on the substrate, leading to enhanced efficiency compared to previously reported bubble-based acoustic micromixers. Additionally, the micromixer can provide efficient mixing under static and continuous flow conditions with further capabilities such as modularity, augmented static volume range and the ability to individually-address different mixers integrated within a common substrate.

The micromixer is fabricated using a combination of rapid prototyping technologies that are low-cost and widely available, enabling quick implementation and broad accessibility. Researchers can reproduce this kind of micromixers with minimal equipment and without the need for trained technicians, expensive equipment and complex facilities as required in the devices fabricated using (SU-8 mould) soft-lithography. The mixer module is highly versatile, it can be integrated into practically any substrate, here we demonstrated implementation with a PMMA layer-by-layer approach and two 3D-printing techniques. The use of a pick-and-place approach can be envisaged to place the elastomeric slab onto moulded chips in a mass-manufacturing setting, following a similar disposable chip concept as shown in Fig. S1.†

We have demonstrated the capability of the hybrid micromixer to significantly outperform the bench protocol for cfDNA extraction in 100 μl plasma samples using a commercial kit based on magnetic beads. For 500 μl plasma samples, the micromixer performed as well as the bench protocol.

We envision that the presented concept will help both industrial and academic developments by catalysing the development of innovative solutions in the lab-on-a-chip field.

Ethical statement

Human blood was obtained from healthy volunteers. Samples were used after obtaining donor consents. Ethical clearance was obtained from the UK National Health Service, East of Scotland Research Ethics Service, reference 19/ES/0056, and Heriot-Watt University EPS Ethics Committee, reference 19/EA/MKK/1.

Author contributions

A. J. C. conceived the concept and fabricated the devices. A. J. C. and A. O. and performed the mixing characterisation experiments. A. J. C. and I. K. performed the biological characterisation experiments. M. K. K. acquired funding, supervised the work and provided ethical clearance. A. J. C. and M. K. K. wrote the manuscript. All co-authors edited the manuscript.

Conflicts of interest

There are no conflicts to declare.

Acknowledgements

We acknowledge EPSRC EP/R00398X/1 for providing the funding necessary to complete this research. We are truly thankful to all our blood donors that kindly volunteered for this experiment.

References

1 G. Cai, L. Xue, H. Zhang and J. Lin, *Micromachines*, 2017, **8**, 274.
2 T. M. Squires and S. R. Quake, *Rev. Mod. Phys.*, 2005, **77**, 977–1026.
3 L.-H. Lu, K. S. Ryu and C. Liu, *J. Microelectromech. Syst.*, 2002, **11**, 462–469.
4 A. R. Shields, B. L. Fiser, B. A. Evans, M. R. Falvo, S. Washburn and R. Superfine, *Proc. Natl. Acad. Sci. U. S. A.*, 2010, **107**, 15670–15675.
5 D. Owen, M. Ballard, A. Alexeev and P. J. Hesketh, *Sens. Actuators, A*, 2016, **251**, 84–91.
6 T. D. Luong, V. N. Phan and N. T. Nguyen, *Microfluid. Nanofluid.*, 2011, **10**, 619–625.
7 I. Iranmanesh, M. Ohlin, H. Ramachandraiah, S. Ye, A. Russom and M. Wiklund, *Biomed. Microdevices*, 2016, **18**, 1–7.
8 H. Van Phan, M. B. Coşkun, M. Şeşen, G. Pandraud, A. Neild and T. Alan, *Lab Chip*, 2015, **15**, 4206–4216.
9 P. H. Huang, Y. Xie, D. Ahmed, J. Rufo, N. Nama, Y. Chen, C. Y. Chan and T. J. Huang, *Lab Chip*, 2013, **13**, 3847–3852.
10 J. van t' Oever, N. Spannenburg, H. Offerhaus, D. van den Ende, J. Herek and F. Mugele, *J. Micro/Nanolithogr., MEMS, MOEMS*, 2015, **14**, 023503.
11 S. Orbay, A. Ozcelik, H. Bachman and T. J. Huang, *J. Micromech. Microeng.*, 2018, **28**, 025012.
12 A. Hashmi, G. Yu, M. Reilly-Collette, G. Heiman and J. Xu, *Lab Chip*, 2012, **12**, 4216–4227.
13 S. Orbay, A. Ozcelik, J. Lata, M. Kaynak, M. Wu and T. J. Huang, *J. Micromech. Microeng.*, 2017, **27**, 1–7.
14 D. Ahmed, X. Mao, B. K. Juluri and T. J. Huang, *Microfluid. Nanofluid.*, 2009, **7**, 727–731.
15 A. Ozcelik, D. Ahmed, Y. Xie, N. Nama, Z. Qu, A. A. Nawaz and T. J. Huang, *Anal. Chem.*, 2014, **86**, 5083–5088.
16 H. Chen, Y. Gao, K. Petkovic, S. Yan, M. Best, Y. Du and Y. Zhu, *Microfluid. Nanofluid.*, 2017, **21**, 30.
17 R. H. Liu, R. Lenigk, R. L. Druyor-Sanchez, J. Yang and P. Grodzinski, *Anal. Chem.*, 2003, **75**, 1911–1917.
18 R. H. Liu, J. Yang, M. Z. Pindera, M. Athavale and P. Grodzinski, *Lab Chip*, 2002, **2**, 151–157.
19 Y. Okabe, Y. Chen, R. Purohit, R. M. Corn and A. P. Lee, *Biosens. Bioelectron.*, 2012, **35**, 37–43.
20 D. Ahmed, X. Mao, J. Shi, B. K. Juluri and T. J. Huang, *Lab Chip*, 2009, **9**, 2738–2741.
21 S. S. Wang, Z. J. Jiao, X. Y. Huang, C. Yang and N. T. Nguyen, *Microfluid. Nanofluid.*, 2009, **6**, 847–852.
22 A. P. Lee, M. V. Patel, A. R. Tovar and Y. Okabe, *JALA*, 2010, **15**, 449–454.
23 M. R. Rasouli and M. Tabrizian, *Lab Chip*, 2019, **19**, 3316–3325.
24 H. Chen, C. Chen, S. Bai, Y. Gao, G. Metcalfe, W. Cheng and Y. Zhu, *Nanoscale*, 2018, **10**, 20196–20206.
25 A. K. Au, W. Lee and A. Folch, *Lab Chip*, 2014, **14**, 1294–1301.
26 A. J. Conde, A. Bianchetti, F. E. Veiras, A. Federico, J. M. Cabaleiro, M. Dufva, R. E. Madrid and L. Fraigi, *RSC Adv.*, 2015, **5**, 49996–50000.
27 A. Liga, J. A. S. Morton and M. Kersaudy-Kerhoas, *Microfluid. Nanofluid.*, 2016, **20**, 1–12.
28 S. Breitbach, S. Tug, S. Helmig, D. Zahn, T. Kubiak, M. Michal, T. Gori, T. Ehlert, T. Beiter and P. Simon, *PLoS One*, 2014, **9**, e87838.
29 C. Chindam, N. Nama, M. Ian Lapsley, F. Costanzo and T. Jun Huang, *J. Appl. Phys.*, 2013, **114**, 194503.
30 A. Marin, M. Rossi, B. Rallabandi, C. Wang, S. Hilgenfeldt and C. J. Kähler, *Phys. Rev. Appl.*, 2015, **3**, 41001.
31 S. Breitbach, S. Tug, P. Simon, R. Primacio, H. Milot, C. Jacob, R. Gyanchandani, E. Kvam, R. Heller, E. Finehout, N. Smith, K. Kota, J. R. Nelson, W. Griffin, S. Puhalla, A. M. Brufsky, N. E. Davidson and A. V. Lee, *J. Preg. Child Health*, 2017, **8**, 4–7.
32 R. Primacio, H. Milot and C. Jacob, *J. Preg. Child Health*, 2017, **4**, 4–7.
33 C. Stemmer, M. Beau-Faller, E. Pencreac'h, E. Guerin, A. Schneider, D. Jaqmin, E. Quoix, M.-P. Gaub and P. Oudet, *Clin. Chem.*, 2003, **49**, 1953–1955.
34 S. Khier and L. Lohan, *Future Sci. OA*, 2018, **4**, FSO295.

